VOT 75155

INVESTIGATING THE FEASIBILITY OF PHOTOGRAMMETRIC AREA-BASED IMAGE MATCHING TECHNIQUE IN THE MEASUREMENT OF THREE-DIMENSIONAL DEFLECTIONS OF STRUCTURES

MUSHAIRRY MUSTAFFAR
AZHAR AHMAD
RADZUAN SA'ARI

PUSAT PENGURUSAN PENYELIDIKAN
UNIVERSITI TEKNOLOGI MALAYSIA

2007

ABSTRACT

INVESTIGATING THE FEASIBILITY OF PHOTOGRAMMETRIC AREA-BASED IMAGE MATCHING TECHNIQUE IN THE MEASUREMENT OF THREE-DIMENSIONAL DEFLECTIONS OF STRUCTURES

(Keywords: Photogrammetry, Beam Deflections, Digital Images, Close-Range, Area-Based Matching)

The study of beam deflections and deformations is one of the many important areas in civil engineering. Designs need to be checked for deflections. The physical behaviour of a structural member subjected to loading provide useful information to structural engineers in deriving optimum designs. Present laboratory practice uses transducers in determining the deflections of beams. These transducers are fitted such that they are physically in contact with the beams. As such, much time is spent in the preparation of the equipment and peripherals for a particular test. Furthermore, deflections can only be measured at points where transducers are fixed and in many cases would be limited. Deflections at any other points, if desired, would be obtained by calculations. This study presents the use of close range digital photogrammetry to obtain a three-dimensional deflections of a concrete beam. Since, photogrammetry has always had the advantage of being able to provide measurements on a large number of points on the object of interest, the representation of the deflections would be enhanced. Image correspondence is achieved by using an area-based image matching which makes use of simple surface models. Laboratory tests involving load test on concrete beams were performed. Images of the beam under various load were captured using off-the-shelf digital cameras that are relatively fixed and calibrated. Whilst the image matching process employs a revised area-based matching algorithm, the image coordinate refinements and the three-dimensional model of the beam's surface was acquired through elementary photogrammetric operations. Validation of the results was done by means of comparing the photogrammetric output against those obtained from the transducers. Initial results show that the differences between the photogrammetric and conventional approaches are not statistically significant. This indicates that the use of close-range digital photogrammetry in producing the deflections is a viable additional approach in determining the physical deformities of concrete structures.

Key Researchers

Assoc. Prof. Dr. Mushairry Mustaffar
Ir. Azhar Ahmad
Radzuan Sa'ari

Tel : 07-5531966
e-mail : mushairry@yahoo.com
Vote No : 75155

1. INTRODUCTION

Analysis on the properties of building structures is a vital procedure in the design of the main structures of any buildings. The proposed frame must be tested in terms of its effectiveness to sustain the designed weight during its serviceable life. Hence, it is obvious that the study of beam structures forms one of the many aspects that has to be dealt with in civil engineering. Various beam properties are investigated, which include among others, shear strength, cracks and deflections, when deciding the numbers of beams required. These computations are normally based on the BS8110 (Mosley, *et. al*., 1999) which stipulates that checks on the deflection of a beam is based on its length and effective depth. Present approach in determining deflections utilizes suitably located electronic transducers (LVDT) or gauges to obtain the magnitude of displacements. Such approach translates to tedious preparatory work and, furthermore, might not be practical to be performed outside the laboratory environment. Moreover, deflections at points without transducers attached are obtained through calculations which are subjected to errors and subsequently affect the final result. A more practical approach that can alleviate some of these problems is by using digital images which are mathematically processed using close-range digital photogrammetry technique.

Photogrammetry has always had the advantage of being a measuring technique that is able to provide an immense number of measured points on the object of interest. The measuring task involves, in essence, the determination of the positions of many conjugate points on a pair of images. In analogue and analytical photogrammetry this task is often considered as laborious due to its repetitive nature. However, the use of digital images in photogrammetry has made it possible to automate this process due to significant developments in computer technology and microelectronics that have taken place in the last few decades. In digital photogrammetry this task is referred to as digital image matching or digital image correlation. As explained by Grün (1996), ever since the conception of the early ideas of digital image matching in the 1950's, great effort has been made to design matching techniques that are more reliable, faster, applicable to various conditions and are able to yield high accuracies.

As far as photogrammetry is concerned, image matching methods can be divided into two groups : feature-based and area-based methods. The former group is fast and reliable and capable of finding matches with poor initial values but its accuracy is limited to approximately the pixel size of the data while the latter approaches have the advantage of high precision (and are able to provide information on the quality of the match). It is the latter group which is of interest here.

Area-based matching utilises a least squares solution of observation equations written for each of the pixels within pre-determined regions surrounding the points to be matched. The observation equation for any one pixel involves the difference in image intensity between that pixel and a

corresponding pixel on the other image. The position of the corresponding pixel is traditionally given by assuming an affine transformation exists between the images. The unknowns to be determined in the solution are the transformation parameters, two of which represent what are conventionally called *x* and *y* parallaxes. No information of the object is taken into account in the matching process. Matching is solely based on the intensity values of the pixels and the assumed affine transformation plus perhaps some radiometric parameters.

1.1 Objectives

The premise behind the study presented in this study is that a number of improvements to the conventional area-based matching theory is possible. This project was therefore undertaken with the aim of developing a method of improving the accuracy of the conventional area-based image matching so that it is viable to be used in determining beam deflections. The need for high accuracies for similar applications in civil engineering has also been the motivation of undertaking this research.

Modifications to the conventional area-based functional model are performed by introducing suitable surface models to describe the relationship between a pair of stereo-images. The conventional affine transformation is replaced by a transformation that uses information of the object surface and the collinearity relationship. In other words, image coordinates of conjugate points on the search image are defined by the image coordinates of the point on the reference image and the corresponding three-dimensional model coordinates (X,Y,Z) on the object as given by the surface model. As with the conventional solution, the method proposed here solves, through an iterative least squares solution the shifts relating to the transformation. New unknowns defining the surface model are also solved.

The performance of the proposed method, in terms of the precision, accuracy and convergence is tested using images of objects with known dimensions. The proposed method presented in this thesis should make a relevant contribution to the area of image matching specifically in civil engineering pertaining to the analysis of structures.

2. BRIEF BACKGROUND OF PHOTOGRAMMETRY

Photogrammetry is the art, science, and technology of obtaining reliable information about physical objects and the environment through the processes of recording, measuring, and interpreting photographic images and patterns of electromagnetic radiant energy and other phenomena. Photogrammetry can also be thought of as the sciences of geometry, mathematics and physics that use the image of a 3D scene on a 2D piece of paper to reconstruct a reliable and accurate model of the original 3D scene. With this in mind it is easier to understand the current expanded definition, which, includes the science of electronics by using video and other synthetic means of reproducing 2D images of 3D scenes. These images are also used to reconstruct reliable and accurate models of the captured 3D scenes. Its most important feature is the fact, that the objects are measured *without being touched*. Therefore, the term "remote sensing" is used by some authors instead of "photogrammetry". Principally, photogrammetry can be divided into close-range (sometimes refered to as terrestrial) and aerial. Aerial photogrammetry is mainly used to produce topographical or thematical maps and digital terrain models. Among the users of close-range photogrammetry are architects and civil engineers (to supervise buildings, document their current state, deformations or damages), archaeologists, surgeons (plastic surgery) or police departments (documentation of traffic accidents and crime scenes), just to mention a few.

2.1 DIGITAL PHOTOGRAMMETRIC MEASUREMENT

As a measuring technique, photogrammetry has always been in the past the laborious manual procedure for gathering information. This has typically involved a photogrammetric operator following contours across the object, and again typically the ground topography seen in the stereoscopic overlap area of a pair of aerial photographs. As many readers will be aware, developments in electronic computing have long ago suggested the possibility of automating this rather repetitive procedure. While automated photogrammetry is not yet perfectly reliable, many objects, and notably terrain from air photographs, can now be measured by procedures which are almost fully automated.

In the case of aerial survey, "digital photogrammetric work-stations", which are, in effect, standard work-stations operating extensive and sophisticated photogrammetric software, available form a small number of manufacturers, are able to carry out relative orientations and digital terrain model generation with complete automation given digitised photographs of terrain meeting certain reasonable criteria for terrain undulation and radiometric texture. With assistance from the digital terrain models (DTM), orthoimages and contours can be automatically and quickly generated. Interior orientation and absolute orientation are partially automated. Generation of a DTM of

satisfactory density and accuracy from a suitable pair of aerial photographs can be achieved at rates of order of 25 points per second. This is achieved through computer programs to carry out the equivalent of placing the "floating mark" on the surface, as operators need to do on analogue and analytical photogrammetric plotters

In non-topographic measurement, automation of measurement of those objects which have been marked with appropriate types of targets is now a highly automated procedure. However, this study is concerned not so much with the finding of targets as with the measurement of surfaces, defined by numerous points found through the automated matching. Although this can often be carried out using the same work-stations intended primarily for aerial photographic use, the peculiarities of non-topographic measurement often mean that it is carried out using cheaper proprietary software loaded onto personal computers or work-stations or software developed in-house such purposes.

The heart of procedures to carry out automated measurement on either aerial or non-aerial imagery remains the software which carries out the "digital image matching", or "image correlation", alluded to above. For this purpose, a number of approaches have been developed over the last few decades. These techniques can be classified into two main groups, feature-based and area-based matching. The former group is fast and reliable and capable of finding matches with poor initial values, while the latter approaches have the advantage of high precision. It is the latter group which is of interest here.

Area-based stereo image matching techniques make use of two small areas (windows) surrounding the point for which matching is needed within each image. A correlation technique, generally based on least squares estimation, selects the point of best match. Methods in area-based matching have developed since early significant, seminal work by Foerstner (1982) and Grün (1985). Further significant extensions of area-based matching were proposed by Grün & Baltsavias (1988); Rosenholm (1987a & 1987b) proposed a method of multi-point area-based matching technique in evaluating three-dimensional models, and area-based method was further extended by Baltsavias (1991) through the use of images from several viewpoints, i.e. with multiple images. Further developments of the area-based method was proposed by Wrobel (1991) and Heipke (1992) in which the matching integrates image matching and object surface reconstruction. Dare (2002) and Fraser & Hanley (2003) have applied area-based matching techniques to satellite imageries.

2.2 REFINEMENT OF THE STANDARD AREA-BASED IMAGE MATCHING MODEL USING A SURFACE MODEL

Mathematical details of conventional area-based matching are provided in many publications (e.g. see Mitchell, 1991 for a review) and are not given here. It may be sufficient to point out that ABM is based

on least squares solution of a number of similar equations, one being written for each pixel in the selected "window" surrounding the point to be matched on one image. The equation for any pixel incorporates the image co-ordinates in one window and the image co-ordinates of corresponding pints in the other window, via a transformation equation. Conventionally, an affine transformation between the windows is adopted. The unknowns to be determined in the least squares solution are the parameters defining this transformation - including parameters which define the relative positions of the windows. In effect, these parameters represent what are conventionally called x and y parallaxes. The equations often also incorporate radiometric values but these are not significant to this brief explanation. No information of the object is taken into account in the matching process. Matching is solely based on the intensity values of the pixels and the assumed affine transformation.

An attempt has been made to improve the accuracy of the traditional area-based technique as offered by Grün (1996). The revision involves replacing the conventional model which is used to transform one window shape to the other to improve the mathematical description of the relationship between the windows in the least squares fit. The new transformation incorporates a simple model of the surface being measured, and replaces the assumption that the windows differ according to an affine transformation. It serves as a compromise between the traditional and the far more complex global area-based matching method. As with the conventional solution, the method proposed here solves, through an iterative least squares solution, for the corrections to image co-ordinates (x,y) of the search window. But, in addition, two 'new' unknowns, the gradients in X and Y directions on the surface at the point on the surface which corresponds to the centre of the search window and their second derivatives are introduced.

Since the transformation used is more rigorous than the affine, it is hypothesised that the improved functional model will allow the use of larger windows for matching and hence improve accuracy. It is also found that the use of a better functional model will converge more quickly to give a solution.

3. AREA-BASED MATCHING USING SURFACE MODELS

The basic area-based observation equation, which gives a relationship between the radiometric values of corresponding pixels in the left and right image, can be written as follows :-

$$I_L(x_L, y_L) + n(x,y) = I_R(x_R, y_R) \quad \text{... 3.1(a)}$$

where,

I_L, I_R are the intensities of the left and right pixel respectively

x_L, y_L are the image coordinates of the left pixel

x_R, y_R are the corresponding image coordinates on the right image

$n(x,y)$ is the difference caused by noise at the point (x_L,y_L) on the left image.

If the relationship between image coordinates on the left (x_L,y_L) and (x_R,y_R) on the right is traditionally given by assuming an affine transformation exists between the images, then matching has to be done using only those pixels in those sub-areas of the images in which the affine relationship still holds between the two images.

The sub-area's coordinate system is a local system defined to perform the affine transformation and is different from the image's coordinate system. In other words, two coordinate systems are essential : a local system to base the affine transformation on and an overall system for the whole image to define the pixel positions and their grey level values.

The use of an affine transformation in representing the relationships between the two images also means that no information of the object is taken into account in the matching process. However, if a projective condition such as the collinearity conditions and the object's shape are used, a greater fidelity is involved in the transformation between the two images. Moreover, if some information about the surface to be measured is available then some sensible surface model can be introduced and the problem could be alleviated. Matching can then be constrained to the geometrical properties of the model, viz., information of the object surface itself. In doing so, image coordinates (x_R,y_R) are expressed in terms of (x_L,y_L) using coordinates (X,Y,Z) on the object surface.

Consider a window of size $n \times n$ pixels on the left image with its centre (i.e. the central pixel) having the coordinates of (x_L,y_L). It should be noted that, the 'central pixel' does not necessarily have to be the centre of the window and that the window does not have to be a square. These circumstances are chosen merely for the convenience of explanation. Introducing a surface model would enable us to represent (x_R,y_R), which are not necessarily integers, on the right image in terms of the central pixel

(point) on the left (x_L,y_L) and the corresponding coordinates (X_o,Y_o,Z_o) on the surface. Apart from the central point, the relationships of neighbouring points, say, ($x_L+\Delta x_L$, $y_L+\Delta y_L$) on the left image and ($x_R+\Delta x_R$, $y_R+\Delta y_R$) are also needed. The shifts Δx_R and Δy_R are related to Δx_L and Δy_L by the surface model. It is evident, at this stage, that values Δx_L and Δy_L are known (these shifts are selected) while Δx_R and Δy_R are not known.

Using the collinearity equations means that three additional parameters, (X,Y,Z) will be introduced for the central pixel and also for each of the neighbouring points. Supposing that the six relative orientation parameters of the cameras or sensors are precisely known, then a simpler relationship of the points used that relates to the object coordinates (X,Y,Z) can be obtained through the epipolar constraint. To do this, a deterministic mathematical model is adopted for the surface, such that coordinates of neighbouring points on the surface, say, (X_p,Y_p,Z_p) are related to the central point (X_o,Y_o,Z_o).

3.1 Mathematical Background

One of the main tasks needed now is to establish the relationship between the neighbouring points and the central point of the window. Assuming that the refined coordinates (i.e with corrections to lens distortion applied) of the central point of the window on the left image is given by (x_L,y_L), then, through the use of the collinearity conditions, the following applies :-

$$x_L = f_{x_L}(X_o,Y_o,Z_o) \qquad \text{... 3.1(b)}$$

$$y_L = f_{y_L}(X_o,Y_o,Z_o) \qquad \text{... 3.1(c)}$$

where,

x_L,y_L are the known coordinates of the central point on the left image
X_o,Y_o,Z_o are the corresponding object space coordinates of the central point
f_{x_L} , f_{y_L} are the collinearity conditions

The object space coordinates (X_o,Y_o,Z_o) are not known, but needed. Initial or provisional values could be estimated using the observed image coordinates (i.e. central point) on both the left and right windows and the collinearity condition. If the neighbouring points within the left window are represented by shifts $(\Delta x_L, \Delta y_L)$ from the central point in *x* and *y* directions respectively, then Eqn. 3.1 (b) and (c) can be written as :-

$$x_L + \Delta x_L = f_{x_L}(X_p, Y_p, Z_p) \quad \text{... 3.2(a)}$$

$$y_L + \Delta y_L = f_{y_L}(X_p, Y_p, Z_p) \quad \text{... 3.2(b)}$$

where (X_p, Y_p, Z_p) are the object space coordinates of the neighbouring points. If the differences between the central point coordinates (X_o, Y_o, Z_o) and (X_p, Y_p, Z_p) are given by ΔX, ΔY and ΔZ in the X, Y and Z directions, then (X_p, Y_p, Z_p) can be expressed in terms of (X_o, Y_o, Z_o), i.e :-

$$X_p = X_o + \Delta X \quad \text{... 3.3(a)}$$

$$Y_p = Y_o + \Delta Y \quad \text{... 3.3(b)}$$

$$Z_p = Z_o + \Delta Z \quad \text{... 3.3(c)}$$

Equation 3.2 can now be rewritten as :-

$$x_L + \Delta x_L = f_{x_L}(X_o + \Delta X, Y_o + \Delta Y, Z_o + \Delta Z) \quad \text{... 3.4(a)}$$

$$y_L + \Delta y_L = f_{y_L}(X_o + \Delta X, Y_o + \Delta Y, Z_o + \Delta Z) \quad \text{... 3.4(b)}$$

3.2 First Order (Planar) Surface Model

Supposing that matching is to be done for a flat surface, then a planar (first order) surface model can now be introduced across the window to represent the surface (see Fig. 3.1). The change of elevation (ΔZ) at any point on the surface is given by :-

$$\Delta Z = \frac{\partial Z}{\partial X}\Delta X + \frac{\partial Z}{\partial Y}\Delta Y \quad \text{... 3.5}$$

where $(\partial Z/\partial X)$ and $(\partial Z/\partial Y)$ are the gradients of Z in X and Y directions respectively. These gradients define the model surface and they are to be evaluated in the solution. The changes in X and Y (i.e. the terms ΔX and ΔY) can be expressed as a function of the corresponding shifts on the left image, Δx_L and Δy_L respectively, as follows :-

$$\Delta X = \frac{\partial X}{\partial x_L}\Delta x_L + \frac{\partial X}{\partial y_L}\Delta y_L \quad \text{... 3.6}$$

$$\Delta Y = \frac{\partial Y}{\partial x_L}\Delta x_L + \frac{\partial Y}{\partial y_L}\Delta y_L \qquad \text{... 3.7}$$

Substituting Eqns. 3.6 and 3.7 into Eqn. 3.5 would yield :-

$$\Delta Z = \frac{\partial Z}{\partial X}\left(\frac{\partial X}{\partial x_L}\Delta x_L + \frac{\partial X}{\partial y_L}\Delta y_L\right) + \frac{\partial Z}{\partial Y}\left(\frac{\partial Y}{\partial x_L}\Delta x_L + \frac{\partial Y}{\partial y_L}\Delta y_L\right) \qquad \text{... 3.8}$$

where,

$\frac{\partial X}{\partial x_L}, \frac{\partial X}{\partial y_L}, \frac{\partial Y}{\partial x_L}, \frac{\partial Y}{\partial y_L}$ are derived from the collinearity equations

Δx_L and Δy_L are preselected shifts on the left image (typically, integer number of pixels)

This implies that, ΔX, ΔY and ΔZ can be written in terms of the known shifts Δx_L and Δy_L, as well as the surface gradient $(\partial Z/\partial X)$ and $(\partial Z/\partial Y)$. Since, ΔX, ΔY,ΔZ, $(\partial Z/\partial X)$ and $(\partial Z/\partial Y)$ represent the planar surface model, these terms are common to both the left and right image. In other words, if a point on the left image whose coordinates are $(x_L+\Delta x_L, y_L+\Delta y_L)$ was selected, then it is possible to estimate the corresponding coordinates on the right $(x_R+\Delta x_R, y_R+\Delta y_R)$ via the planar surface model. Thus the conventional area based matching observation equation (see Eqn. 3.1(a)) can now be expanded to represent neighbouring points by :-

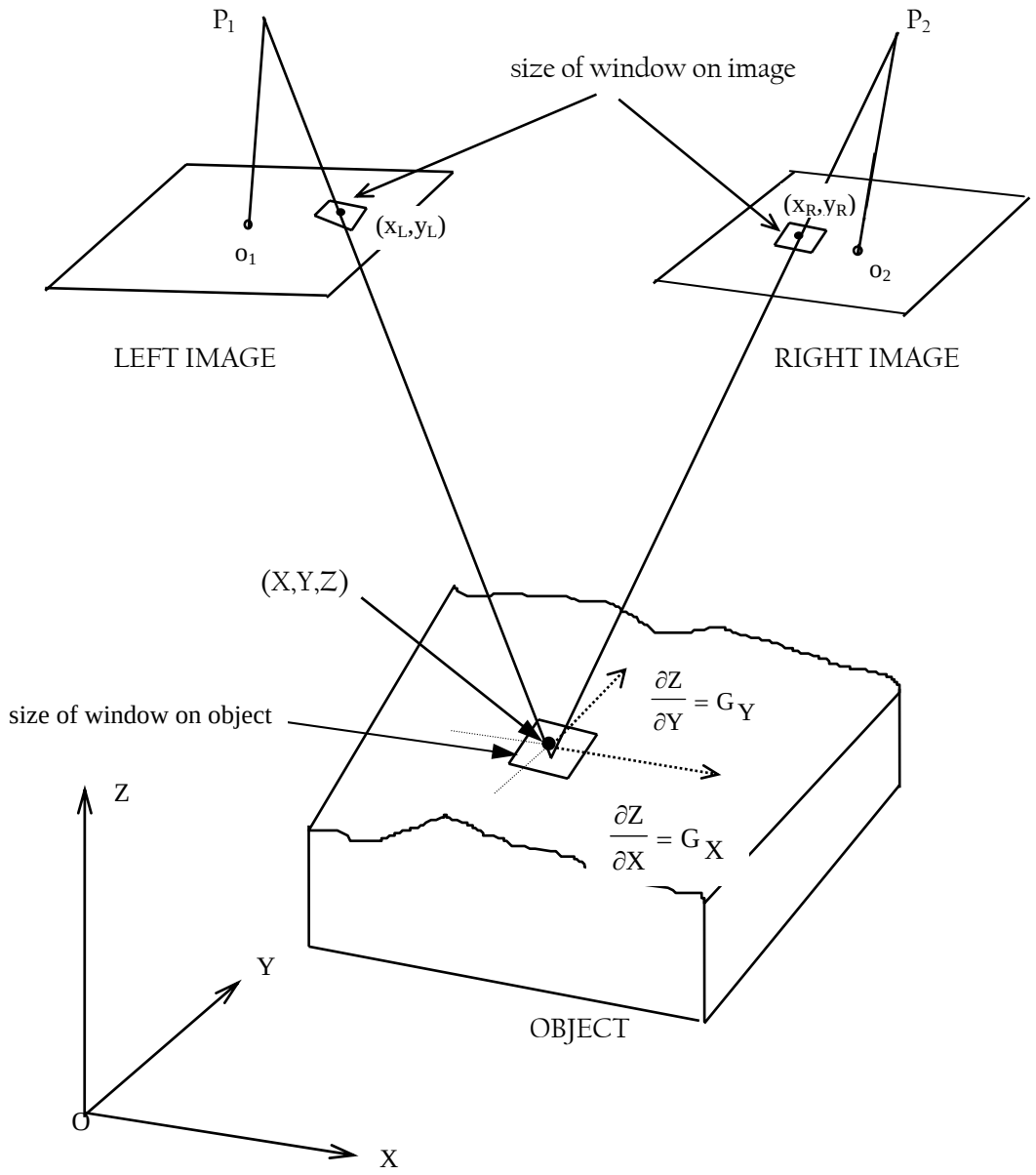

Figure 3.1 Diagram showing the use of object's surface gradients G_X and G_Y in area based matching. Points P_1 and P_2 are the perspective centre of the cameras whereas o_1 and o_2 are the principal points.

$$I_L(x_L+\Delta x_L, y_L+\Delta y_L) + n(x+\Delta x, y+\Delta y) = I_R(x_R+\Delta x_R, y_R+\Delta y_R) \quad \text{... 3.9}$$

The terms Δx_R and Δy_R which represent the unknown shifts on the right window can be expressed in terms of the known shifts, Δx_L and Δy_L, on the left image and the known shift on the object, ΔX, ΔY,ΔZ, via the planar surface model. Firstly, let us consider the term Δx_R, which can be expressed as :-

$$\Delta x_R = \frac{\partial x_R}{\partial X}\Delta X + \frac{\partial x_R}{\partial Y}\Delta Y + \frac{\partial x_R}{\partial Z}\Delta Z \quad \text{... 3.10}$$

Substituting Eqns. 3.6 to 3.8 into Eqn. 3.10 will give :-

$$\Delta x_R = \frac{\partial x_R}{\partial X}\left(\frac{\partial X}{\partial x_L}\Delta x_L + \frac{\partial X}{\partial y_L}\Delta y_L\right) + \frac{\partial x_R}{\partial Y}\left(\frac{\partial Y}{\partial x_L}\Delta x_L + \frac{\partial Y}{\partial y_L}\Delta y_L\right)$$

$$+ \frac{\partial x_R}{\partial Z}\left\{G_X\left(\frac{\partial X}{\partial x_L}\Delta x_L + \frac{\partial X}{\partial y_L}\Delta y_L\right) + G_Y\left(\frac{\partial Y}{\partial x_L}\Delta x_L + \frac{\partial Y}{\partial y_L}\Delta y_L\right)\right\}$$

... 3.11

where $(\partial Z/\partial X)$ and $(\partial Z/\partial Y)$ are replaced by G_X and G_Y respectively. It should be noted that these terms define the surface model. The term Δx_R can be expressed in terms of Δx_L, Δy_L, G_X and G_Y as :-

$$\Delta x_R = \left(\frac{\partial x_R}{\partial X}\cdot\frac{\partial X}{\partial x_L} + \frac{\partial x_R}{\partial Y}\cdot\frac{\partial Y}{\partial x_L}\right)\Delta x_L + \left(\frac{\partial x_R}{\partial X}\cdot\frac{\partial X}{\partial y_L} + \frac{\partial x_R}{\partial Y}\cdot\frac{\partial Y}{\partial y_L}\right)\Delta y_L$$

$$+ \left(\frac{\partial x_R}{\partial Z}\cdot\frac{\partial X}{\partial x_L}\Delta x_L + \frac{\partial x_R}{\partial Z}\cdot\frac{\partial X}{\partial y_L}\Delta y_L\right)G_X + \left(\frac{\partial x_R}{\partial Z}\cdot\frac{\partial Y}{\partial x_L}\Delta x_L + \frac{\partial x_R}{\partial Z}\cdot\frac{\partial Y}{\partial y_L}\Delta y_L\right)G_Y$$

... 3.12

Eqn. 3.12 expresses Δx_R in terms of the known shifts Δx_L , Δy_L on the left image, the partial derivatives of the collinearity equations (calculated using provisional values of x_R^o, y_R^o and computed X_O, Y_O, Z_O) and the terms G_X, G_Y as obtained from the planar surface model. As such, only G_X and G_Y are not known and need to be solved. Introducing $d\Delta x_R$, dG_X, dG_Y for linearising purposes :-

$$d\Delta x_R = \frac{\partial \Delta x_R}{\partial G_X} dG_X + \frac{\partial \Delta x_R}{\partial G_Y} dG_Y \qquad \text{... 3.13}$$

The partial derivatives $(\partial \Delta x_R/\partial G_X)$ and $(\partial \Delta x_R/\partial G_Y)$ are obtainable from Eqn. 3.12, and are :-

$$\frac{\partial \Delta x_R}{\partial G_X} = \frac{\partial x_R}{\partial Z} \cdot \frac{\partial X}{\partial x_L} \Delta x_L + \frac{\partial x_R}{\partial Z} \cdot \frac{\partial X}{\partial y_L} \Delta y_L \qquad \text{... 3.14a}$$

$$\frac{\partial \Delta x_R}{\partial G_Y} = \frac{\partial x_R}{\partial Z} \cdot \frac{\partial Y}{\partial x_L} \Delta x_L + \frac{\partial x_R}{\partial Z} \cdot \frac{\partial Y}{\partial y_L} \Delta y_L \qquad \text{... 3.14b}$$

Similarly, the relationships for Δy_R and $d\Delta y_R$ are given by :-

$$\Delta y_R = \left(\frac{\partial y_R}{\partial X} \cdot \frac{\partial X}{\partial x_L} + \frac{\partial y_R}{\partial Y} \cdot \frac{\partial Y}{\partial x_L} \right) \Delta x_L + \left(\frac{\partial y_R}{\partial X} \cdot \frac{\partial X}{\partial y_L} + \frac{\partial y_R}{\partial Y} \cdot \frac{\partial Y}{\partial y_L} \right) \Delta y_L + \left(\frac{\partial y_R}{\partial Z} \cdot \frac{\partial X}{\partial x_L} \Delta x_L + \frac{\partial y_R}{\partial Z} \cdot \frac{\partial X}{\partial y_L} \Delta y_L \right) G_X + \left(\frac{\partial y_R}{\partial Z} \cdot \frac{\partial Y}{\partial x_L} \Delta x_L + \frac{\partial y_R}{\partial Z} \cdot \frac{\partial Y}{\partial y_L} \Delta y_L \right) G_Y \qquad \text{... 3.15}$$

$$d\Delta y_R = \frac{\partial \Delta y_R}{\partial G_X} dG_X + \frac{\partial \Delta y_R}{\partial G_Y} dG_Y \qquad \text{... 3.16}$$

and

$$\frac{\partial \Delta y_R}{\partial G_X} = \frac{\partial y_R}{\partial Z} \cdot \frac{\partial X}{\partial x_L} \Delta x_L + \frac{\partial y_R}{\partial Z} \cdot \frac{\partial X}{\partial y_L} \Delta y_L \qquad \text{... 3.17a}$$

$$\frac{\partial \Delta y_R}{\partial G_Y} = \frac{\partial y_R}{\partial Z} \cdot \frac{\partial Y}{\partial x_L} \Delta x_L + \frac{\partial y_R}{\partial Z} \cdot \frac{\partial Y}{\partial y_L} \Delta y_L \quad \text{... 3.17b}$$

The units of the shifts Δx_R and Δy_R could either be millimetres or pixels. This implies that the partial derivatives should be evaluated using appropriate units. For reason explained in section 4.9.1 the units used for all experiments were millimetres. Partial derivatives ($\partial x_R/\partial Z$), ($\partial y_R/\partial Z$), ($\partial x_L/\partial X$), ($\partial y_L/\partial X$), ($\partial x_L/\partial Y$) and ($\partial y_L/\partial Y$) can be obtained from the linearisation of the collinearity equation and are well documented in most photogrammetric books (e.g. Wolf, 1988). They are given by :-

$$\frac{\partial x_R}{\partial Z} = \frac{x_R}{q} m_{33}^R + \frac{f}{q} m_{13}^R \quad \text{... 3.17c}$$

$$\frac{\partial y_R}{\partial Z} = \frac{y_R}{q} m_{33}^R + \frac{f}{q} m_{23}^R \quad \text{... 3.17d}$$

$$\frac{\partial x_L}{\partial X} = \frac{x_L}{q} m_{31}^L + \frac{f}{q} m_{11}^L \quad \text{... 3.17e}$$

$$\frac{\partial x_L}{\partial Y} = \frac{x_L}{q} m_{32}^L + \frac{f}{q} m_{12}^L \quad \text{... 3.17f}$$

$$\frac{\partial y_L}{\partial X} = \frac{y_L}{q} m_{31}^L + \frac{f}{q} m_{21}^L \quad \text{... 3.17g}$$

$$\frac{\partial y_L}{\partial Y} = \frac{y_L}{q} m_{32}^L + \frac{f}{q} m_{22}^L \quad \text{... 3.17h}$$

where m_{13}^R ... m_{33}^R and m_{11}^L ... m_{32}^L are the rotation elements for the right and left image respectively, f is the principal distance and q is given by :-

$$q = m_{31}(X-X_O) + m_{32}(Y-Y_O) + m_{33}(Z-Z_O) \quad \text{... 3.18}$$

Therefore, the partial derivatives that occur in the planar surface model, as shown in Eqn. 3.8 are the reciprocals of Eqns. 3.17e to 3.17h as evaluated on the left image. Linearising Eqn. 3.9 would yield :-

$$I_L\left(x_L + \Delta x_L, y_L + \Delta y_L\right) + n\left(x + \Delta x, y + \Delta y\right) = I_R^o\left(x_R^o + \Delta x_R^o, y_R^o + \Delta y_R^o\right)$$

$$+\left(\frac{\partial I_R}{\partial y_R}\right)dx_R + \left(\frac{\partial I_R}{\partial y_R}\right)dy_R + \left(\frac{\partial I_R}{\partial x_R}\right)d\Delta x_R + \left(\frac{\partial I_R}{\partial y_R}\right)d\Delta y_R \qquad \ldots 3.19$$

where the superscript ^{o} indicates *a priori* estimate and dx_R, dy_R, $d\Delta x_R$ and $d\Delta y_R$ are the corrections to the *a priori* value. Estimates of x_R^o and y_R^o can be obtained from a suitable method, such as a two-dimensional epipolar search of a feature or even manual selection, and estimates of Δx_R^o and Δy_R^o are computed using provisional values of X_O, Y_O, Z_O, $(\partial Z/\partial X)$, $(\partial Z/\partial Y)$ and the planar surface model. The terms $\partial I_R/\partial x_R$ and $\partial I_R/\partial y_R$ are the gradients of the intensities in the *x* and *y* directions across the right image.

Substituting Eqns. 3.13 and 3.16 into Eqn. 3.19 would yield the following linearised observation equation :-

$$I_L\left(x_L + \Delta x_L, y_L + \Delta y_L\right) + n(x + \Delta x, y + \Delta y) = I_R^o\left(x_R^o + \Delta x_R^o, y_R^o + \Delta y_R^o\right)$$

$$+\left(\frac{\partial I_R}{\partial x_R}\right)dx_R + \left(\frac{\partial I_R}{\partial y_R}\right)dy_R + \left(\frac{\partial I_R}{\partial x_R}\cdot\frac{\partial \Delta x_R}{\partial G_X} + \frac{\partial I_R}{\partial y_R}\cdot\frac{\partial \Delta y_R}{\partial G_X}\right)dG_X$$

$$+\left(\frac{\partial I_R}{\partial x_R}\cdot\frac{\partial \Delta x_R}{\partial G_Y} + \frac{\partial I_R}{\partial y_R}\cdot\frac{\partial \Delta y_R}{\partial G_Y}\right)dG_Y \qquad \ldots 3.20$$

Equation 3.20 is linear in dx_R, dy_R, dG_X and dG_Y, and because of the approximations in the linearisation an iterative solution is needed to solve for the corrections to these unknowns. The partial derivatives in G_X and G_Y are evaluated via the surface model using the known values of the cameras' relative orientations.

3.3 Solution of the Observation Equations

The solutions of observation Equations 3.20, as mentioned in the preceding sections, are obtained through an iterative least squares adjustment. Each point (pixel) in the window yields an observation

equation, thus, an $n \times n$ window will result in a set of n^2 observation equations. In matrix notation, the solution can be represented as follows (considering only the planar surface model) :-

$$\mathbf{A}\mathbf{x} + \mathbf{b} = \mathbf{v} \qquad \ldots 3.21$$

where the matrices,

$$\mathbf{A} = \begin{bmatrix} 1 & I_R\left(x_R + \Delta x_R, y_R + \Delta y_R\right)^{(1)} & \left(\frac{\partial I_R}{\partial x_R}\right)^{(1)} r_2 & \left(\frac{\partial I_R}{\partial y_R}\right)^{(1)} r_2 & M^{(1)} r_2 & N^{(1)} r_2 \\ 1 & I_R\left(x_R + \Delta x_R, y_R + \Delta y_R\right)^{(2)} & \left(\frac{\partial I_R}{\partial x_R}\right)^{(2)} r_2 & \left(\frac{\partial I_R}{\partial y_R}\right)^{(2)} r_2 & M^{(2)} r_2 & N^{(2)} r_2 \\ : & : & : & : & : & : \\ : & : & : & : & : & : \\ : & : & : & : & : & : \\ 1 & I_R\left(x_R + \Delta x_R, y_R + \Delta y_R\right)^{(n)} & \left(\frac{\partial I_R}{\partial x_R}\right)^{(n)} r_2 & \left(\frac{\partial I_R}{\partial y_R}\right)^{(n)} r_2 & M^{(n)} r_2 & N^{(n)} r_2 \end{bmatrix} \qquad \ldots 3.22$$

$$\mathbf{x}^{\mathrm{T}} = \begin{bmatrix} \mathrm{dr}_1 & \mathrm{dr}_2 & \mathrm{dx}_{\mathrm{R}} & \mathrm{dy}_{\mathrm{R}} & \mathrm{dG}_{\mathrm{X}} & \mathrm{G}_{\mathrm{Y}} \end{bmatrix} \qquad \ldots 3.23$$

$$\mathbf{b} = \begin{bmatrix} \mathrm{r}_1^{\mathrm{o}} + \mathrm{r}_2^{\mathrm{o}} \mathrm{I}_{\mathrm{R}}\left(\mathrm{x}_{\mathrm{R}} + \Delta \mathrm{x}_{\mathrm{R}}, \mathrm{y}_{\mathrm{R}} + \Delta \mathrm{y}_{\mathrm{R}}\right)^{\mathrm{o}(1)} - \mathrm{I}_{\mathrm{L}}\left(\mathrm{x}_{\mathrm{L}} + \Delta \mathrm{x}_{\mathrm{L}}, \mathrm{y}_{\mathrm{L}} + \Delta \mathrm{y}_{\mathrm{L}}\right)^{(1)} \\ \mathrm{r}_1^{\mathrm{o}} + \mathrm{r}_2^{\mathrm{o}} \mathrm{I}_{\mathrm{R}}\left(\mathrm{x}_{\mathrm{R}} + \Delta \mathrm{x}_{\mathrm{R}}, \mathrm{y}_{\mathrm{R}} + \Delta \mathrm{y}_{\mathrm{R}}\right)^{\mathrm{o}(2)} - \mathrm{I}_{\mathrm{L}}\left(\mathrm{x}_{\mathrm{L}} + \Delta \mathrm{x}_{\mathrm{L}}, \mathrm{y}_{\mathrm{L}} + \Delta \mathrm{y}_{\mathrm{L}}\right)^{(2)} \\ : \\ : \\ : \\ \mathrm{r}_1^{\mathrm{o}} + \mathrm{r}_2^{\mathrm{o}} \mathrm{I}_{\mathrm{R}}\left(\mathrm{x}_{\mathrm{R}} + \Delta \mathrm{x}_{\mathrm{R}}, \mathrm{y}_{\mathrm{R}} + \Delta \mathrm{y}_{\mathrm{R}}\right)^{\mathrm{o}(n)} - \mathrm{I}_{\mathrm{L}}\left(\mathrm{x}_{\mathrm{L}} + \Delta \mathrm{x}_{\mathrm{L}}, \mathrm{y}_{\mathrm{L}} + \Delta \mathrm{y}_{\mathrm{L}}\right)^{(n)} \end{bmatrix} \qquad \ldots 3.24$$

and the terms :-

$$\mathrm{M} = \left(\frac{\partial \mathrm{I}_{\mathrm{R}}}{\partial \mathrm{x}_{\mathrm{R}}} \cdot \frac{\partial \Delta \mathrm{x}_{\mathrm{R}}}{\partial \mathrm{G}_{\mathrm{X}}} + \frac{\partial \mathrm{I}_{\mathrm{R}}}{\partial \mathrm{y}_{\mathrm{R}}} \cdot \frac{\partial \Delta \mathrm{y}_{\mathrm{R}}}{\partial \mathrm{G}_{\mathrm{X}}}\right) \quad ; \quad \mathrm{N} = \left(\frac{\partial \mathrm{I}_{\mathrm{R}}}{\partial \mathrm{x}_{\mathrm{R}}} \cdot \frac{\partial \Delta \mathrm{x}_{\mathrm{R}}}{\partial \mathrm{G}_{\mathrm{Y}}} + \frac{\partial \mathrm{I}_{\mathrm{R}}}{\partial \mathrm{y}_{\mathrm{R}}} \cdot \frac{\partial \Delta \mathrm{y}_{\mathrm{R}}}{\partial \mathrm{G}_{\mathrm{Y}}}\right)$$

The superscript *(1), (2) .. (n)* represents the number of points. The solution of the observation equation is given by :-

$$\mathbf{x} = \left(\mathbf{A}^{\mathrm{T}} \mathbf{W} \mathbf{A}\right)^{-1} \left(\mathbf{A}^{\mathrm{T}} \mathbf{W} \mathbf{b}\right) \qquad \ldots 3.25$$

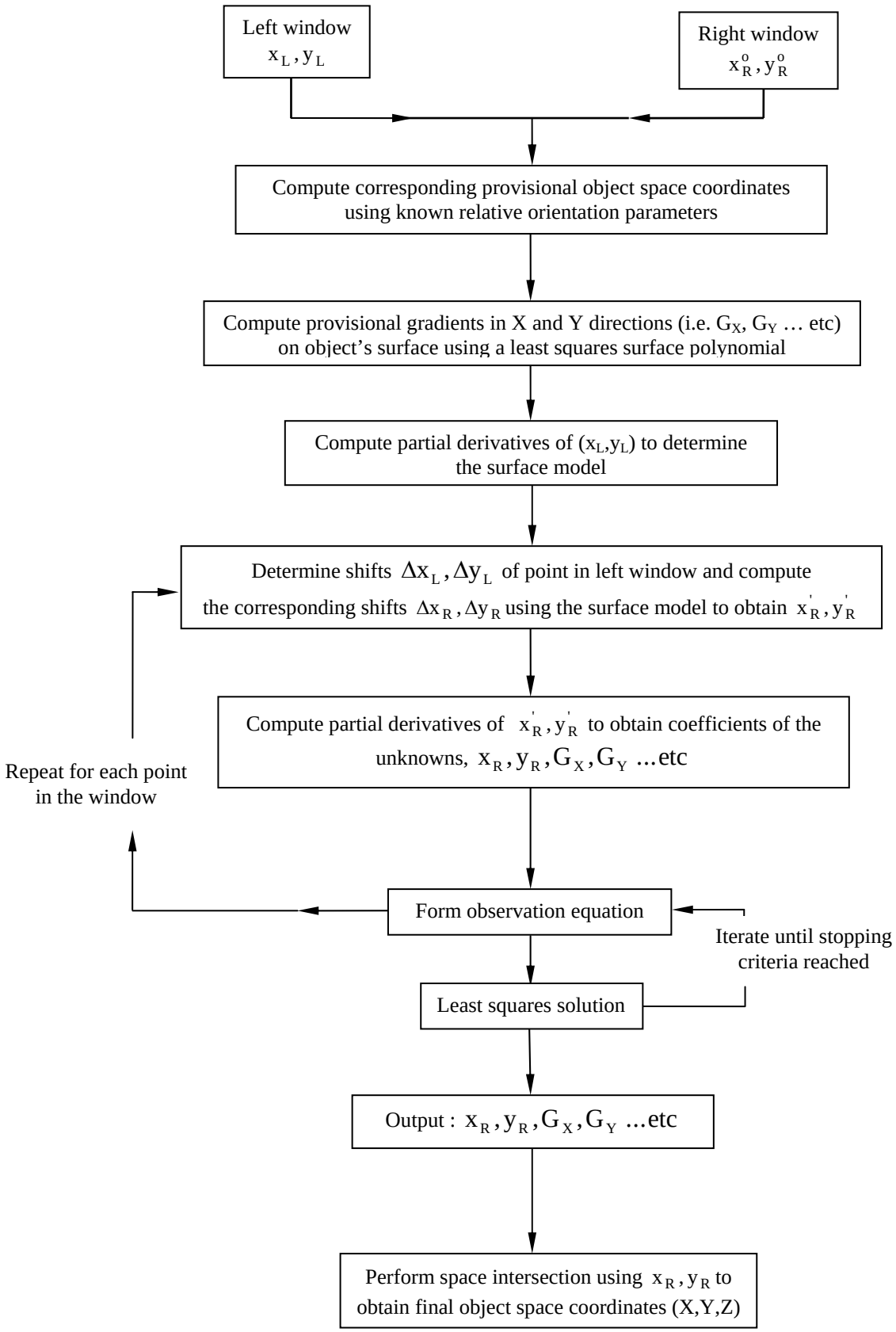

Figure 3.2 Computational steps of the area based matching using a surface model

where the matrix $\mathbf{W}$ is the weight matrix, which in this case is the weight for the intensity (grey level) and as explained in chapter 2 is generally assumed to be an identity matrix. The solution of the method for higher order surface model would follow a similar approach. The size of the matrices $\mathbf{A}$, $\mathbf{x}$ and $\mathbf{b}$ is expanded according to the number of unknowns resulting from the surface model. Figure 3.2 shows the computational procedure of the proposed method schematically.

4. MEASUREMENT OF IMAGES AND COMPUTATIONAL STEPS

A photograph (or digital image) is a perspective projection and the optical centre of the camera is the perspective centre. The region between the perspective centre and the emulsion (in the case of conventional camera) or the sensors (for digital cameras) is called the image space. The region occupied by the object to be imaged, including the reference coordinate system used, is called the object space. Measurements generally involves the transformation from two-dimensional data (coordinates, to be more specific) to three-dimensional output through some perspective relationship.

It is evident that, before any measurements of the images could be taken, *a priori* information pertaining to the geometry and the relative positions of the cameras or sensors is required. This could be achieved by performing the following three vital steps, namely, *interior orientation*, *relative orientation* and *absolute orientation*. (Mustaffar & Mitchell, 2001)

Interior Orientation

The interior orientation of an image defines the form of the bundle of rays emerging from the perspective centre to the points in the object space. The geometrical elements of interior orientation, which are in effect the relative position of the perspective centre and the image coordinate system, are x_o, y_o (coordinate of the perspective centre) and f (focal length of camera).

Exterior Orientation

Exterior orientation of an image defines its position and orientation in the object space. The position of the image is defined by the object space coordinates of the perspective centre. The orientation, which describes the attitude of the camera at the moment of exposure, refers to the spatial relationship between the object coordinate system (X,Y,Z) and the image coordinate system (x,y,z). The most common system for defining the orientation are the orientation angles along each of the three axes.

Absolute Orientation

Absolute orientation refers to the process by which a pair of relatively oriented photographs or images is related to the ground system. In other words, it is the process whereby the three-dimensional model (which is usually obtained analytically using information obtained during the exterior orientation) formed is related to the ground coordinate system.

The above processes are only briefly explained. For more detailed explanation, readers are encouraged to refer to any of the textbooks in photogrammetry (e.g. Wolf, 1988).

4.1 COMPUTATIONS OF OBJECT SPACE COORDINATES (X,Y,Z)

The provisional object space coordinates of the point to be matched are computed using the collinearity equations in conjunction with the image coordinates and the relative orientation parameters. In this project the computation of the object space coordinate are performed to :-

a) evaluate the partial differentials associated with the surface model used,

b) obtain estimates of the object's surface gradients in X and Y directions by fitting a polynomial on the object's surface,

c) compute the final (X,Y,Z) of the matched points.

For an image point whose coordinates are (x, y), the collinearity equation, which can be found in most photogrammetric textbooks, are given by :-

$$x - x_o = -f\left(\frac{m_{11}(X - X_o) + m_{12}(Y - Y_o) + m_{13}(Z - Z_o)}{m_{31}(X - X_o) + m_{32}(Y - Y_o) + m_{33}(Z - Z_o)}\right) \qquad \ldots 4.1$$

$$y - y_o = -f\left(\frac{m_{21}(X - X_o) + m_{22}(Y - Y_o) + m_{23}(Z - Z_o)}{m_{31}(X - X_o) + m_{32}(Y - Y_o) + m_{33}(Z - Z_o)}\right) \qquad \ldots 4.2$$

where,

$m_{11} .. m_{33}$ are elements of the rotation matrix

x_o, y_o are the image coordinates of the principal point

X,Y,Z are the corresponding object space coordinates of (x,y)

X_o, Y_o, Z_o are the object space coordinates of the perspective centre

Eqns 4.1 and 4.2 can be formed for a point in the image. Supposing a pair of corresponding image points is available, then four collinearity equations can be formed and the object coordinates (X,Y,Z) can be directly computed using any three of the equations. If the position of the left camera is held

fixed during the relative orientation process (as in a one-projector relative orientation) then the rotations will result in an identity rotation matrix, i.e. :-

$$\begin{bmatrix} m_{11}^L & m_{12}^L & m_{13}^L \\ m_{21}^L & m_{22}^L & m_{23}^L \\ m_{31}^L & m_{32}^L & m_{33}^L \end{bmatrix} = \begin{bmatrix} 1 & 0 & 0 \\ 0 & 1 & 0 \\ 0 & 0 & 1 \end{bmatrix} = \mathbf{I} \qquad \text{... 4.3}$$

Assume that the object space coordinates are based on the left-hand perspective centre, then $X_o = Y_o = Z_o = 0$ and, for simplicity sake, adopting the coordinates of the principal point $x_o = y_o = 0$. (In practice however, the origin of the image's coordinate system is normally at the top or bottom left corner). Eqns. 4.1 and 4.2 are simplified as follows :-

$$x_L = -f_L \frac{X}{Z} \qquad \text{... 4.4a}$$

$$y_L = -f_L \frac{Y}{Z} \qquad \text{... 4.4b}$$

If the rotation matrix for the right camera is given by :-

$$R^R = \begin{bmatrix} m_{11}^R & m_{12}^R & m_{13}^R \\ m_{21}^R & m_{22}^R & m_{23}^R \\ m_{31}^R & m_{32}^R & m_{33}^R \end{bmatrix} \qquad \text{... 4.5}$$

and the object space coordinates of the perspective centre are $\left(X_o^R, Y_o^R, Z_o^R\right)$ then the collinearity equations for the corresponding point on the right image are given as :-

$$x^R = -f_R \left(\frac{m_{11}^R\left(X - X_o^R\right) + m_{12}^R\left(Y - Y_o^R\right) + m_{13}^R\left(Z - Z_o^R\right)}{m_{31}^R\left(X - X_o^R\right) + m_{32}\left(Y - Y_o^R\right) + m_{33}\left(Z - Z_o^R\right)} \right) \qquad \text{... 4.6}$$

$$y^R = -f_R \left(\frac{m_{21}^R\left(X - X_o^R\right) + m_{22}^R\left(Y - Y_o^R\right) + m_{23}^R\left(Z - Z_o^R\right)}{m_{31}^R\left(X - X_o^R\right) + m_{32}\left(Y - Y_o^R\right) + m_{33}\left(Z - Z_o^R\right)} \right) \qquad \text{... 4.7}$$

It can be readily seen that the object coordinates (X,Y,Z) could be computed by using Eqns. 4.4(a), 4.4(b) 4.6 and 4.7., i.e. 4 equations against 3 unknowns. In other words, a least squares could be performed to solve for the unknowns. However, as described by, e.g. Wolf (1988), van der Merwe

(1995), the computations of the object space coordinates X and Y can be reduced to a 2×2 matrix by substituting either Eqn. 4.4(a) or 4.4(b) into Eqns. 4.6 and 4.7. Since good determination of parallax is achieved in the x direction (i.e. better intersection of the rays) it is best to use Eqn. 4.4(a), 4.6 and 4.7 for computing the object space coordinates. The Z component is then obtained by back substitution into either Eqn. 4.4(a) or 4.4(b). In this project, the latter approach is adopted for the computations of the object space coordinates.

5. TEST CONDUCTED

Two beams of sizes 120 × 250 × 3000 and 160 × 250 × 3000 respectively were fabricated for the test. These beams were mounted on the test rig marked with suitable targets at points where deflections were to be determined. A LVDT was placed at the centre of the beam (aligned with the target marked at the centre of the beam) so that its readings could be directly compared to those obtained photogrammetrically. Images were captured using a digital SLR Nikon D70 cameras that were mounted on a horizontal bar. Figure 5.1 depicts the experimental setup.

Processing of the images was done using a proprietry close range photogrammetry software PhotoModeler Pro 5. Camera was calibrated prior to image measurements using the routines in the software. Figure 5.2(a) and (b) show the calibration template and the calibration setup for each of the camera used respectively.

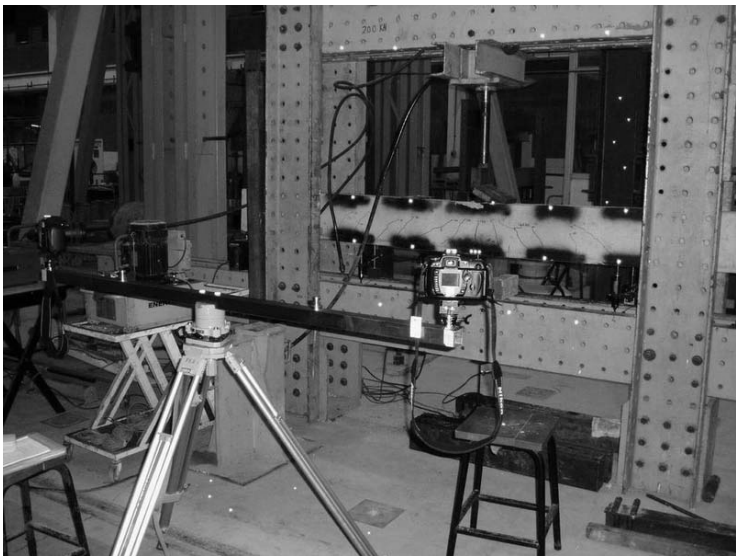

Figure 5.1 Experimental setup

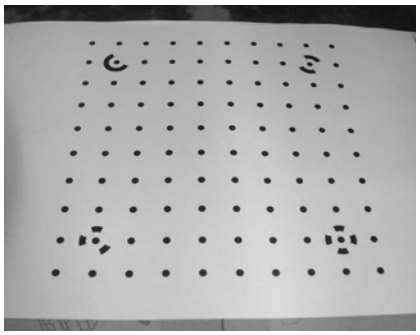

Figure 5.2(a) Calibration Template

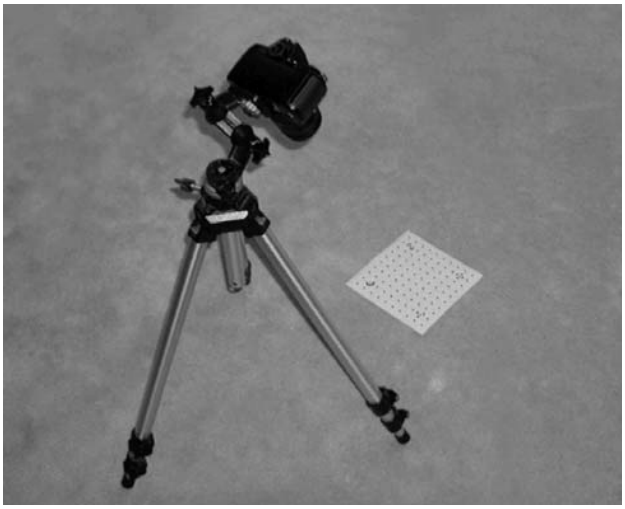

Figure 5.22(b) Calibrating one of the cameras used.

6. RESULTS AND ANALYSIS

The displacements of the points on the beam, which in fact are deflections, are given in terms of 3D coordinates by Photomodeler Pro 5. As explained earlier, only one LVDT was used therefore comparisons can only be made with the target fitted immediately above the sensor on the beam. Table 6.1(a) and (b) show the summary of the results obtained for both beam sizes.

Table 6.1(a) Comparison of deflection magnitudes for Beam size 120 × 250 × 3000

Loading (KN)	LVDT (mm)	Photogrammetry (mm)	Theory (mm)
0	0	0	0.00
10	1.03	1.39	1.70
30	4.25	4.54	5.23
40	5.76	6.09	7.00
60	8.95	9.48	10.45
80	14.18	14.51	13.94
90	17.88	17.83	15.68

Table 6.1(b) Comparison of deflection magnitudes for Beam size 160 × 250 × 3000

Loading (KN)	LVDT (mm)	Photogrammetry (mm)	Theory (mm)
0	0.97	1.71	1.72
30	3.54	4.29	4.51
50	6.17	6.88	7.30
70	8.86	9.34	10.09
100	13.02	13.5	14.27
120	16.62	16.97	17.06
150	28.58	28.48	21.24

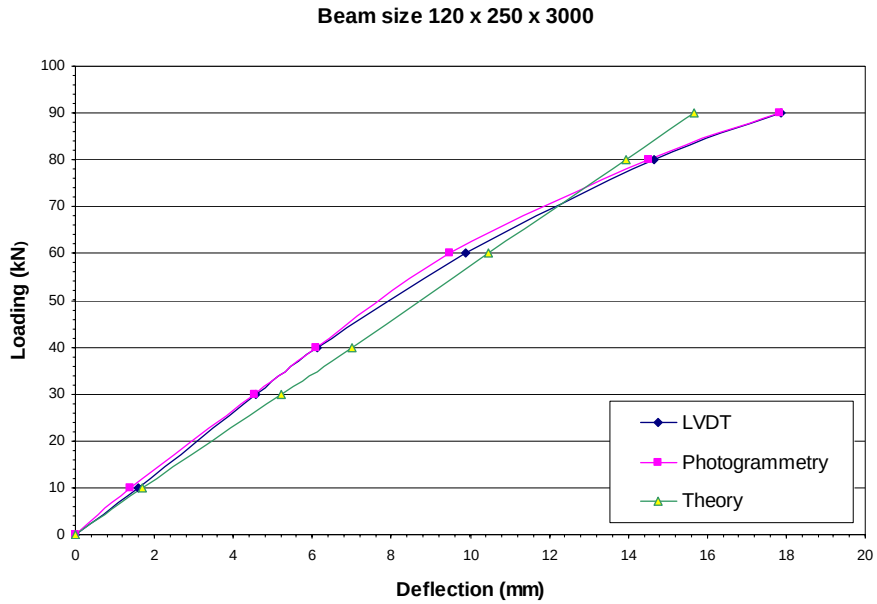

Figure 6.1(a) Graph showing the magnitude of deflections against various loading for beam size 120×250×3000

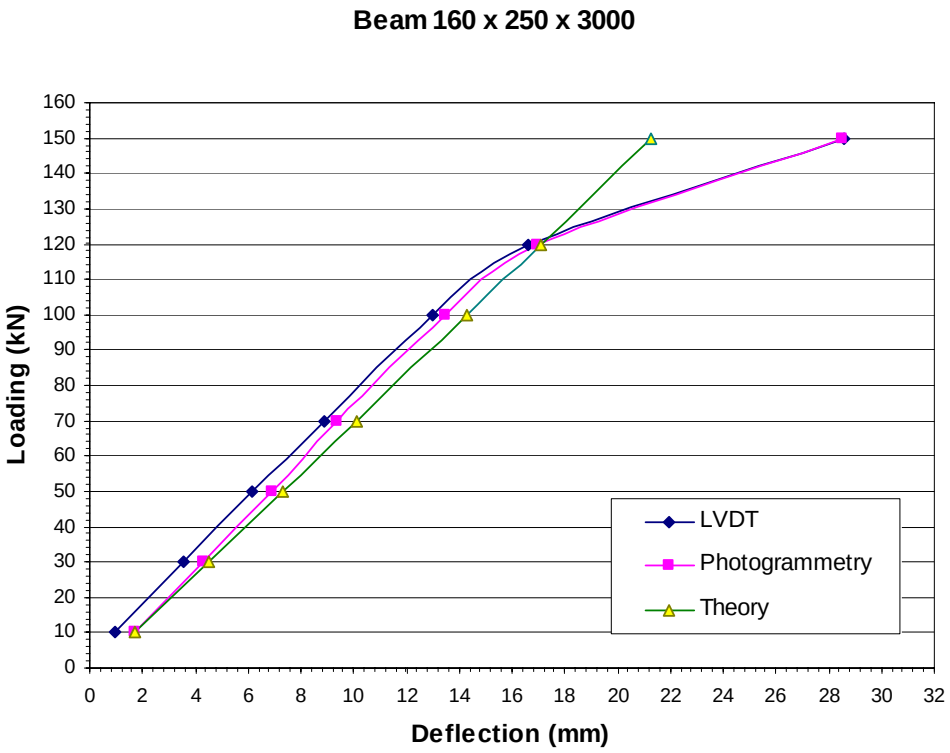

Figure 6.1(b) Graph showing the magnitude of deflections against various loading for beam size 160×250×3000

Figures 6.1(a) and 6.1(b) represent the deflection magnitudes for both beams. It is evident from both figures that the curves representing the photogrammetric output fit better with the LVDT curves as compared to those of the calculation method.

The differences in the deflection magnitudes between those obtained form the LVDT and photogrammetry methods are depicted in Figures 6.2(a) and 6.2(b). A t-test with 95% confidence level (α = 0.5) indicated that the mean difference between LVDT and photogrammetric values are ± 0.35 mm. The standard errors for both beams are found to be not significantly different as revealed by an F-test with the same level of confidence as per the t-test.

Figure 6.2(a) Graph showing the differences in deflections between LVDT and Photograamtery against various loading for beam size 120×250×3000

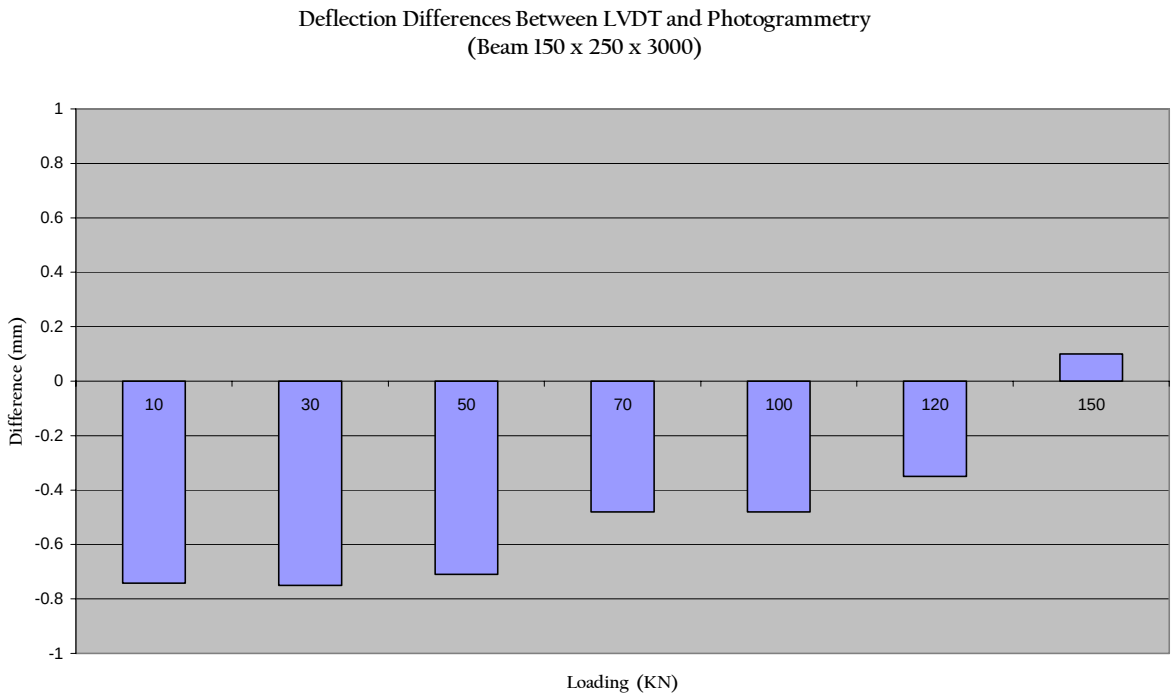

Figure 6.2(b) Graph showing the differences in deflections between LVDT and Photograamtery against various loading for beam size 150×250×3000

7. CONCLUSIONS

This study has shown that digital image measurements using close-range photogrammety can be successfully applied to the measurements of beam deflections. This is clearly indicated by the small differences in the deflections and further strengthened by the statistical test. As this test was done under laboratory conditions it will be fruitful to apply the method outlined for measurements on existing structures under natural light conditions. The method reported here is intended to be used as an additional approach so that structural engineers can be furnished with further information in their analysis of beam deflections.

REFERENCES

Baltsavias, E.P. (1991) **Multiphoto Geometrically Constrained Matching**. Ph.D. thesis, Institute of Geodesy and Photogrammetry, ETH-Zurich. Mitteilungen Nr. 49, 221p

Dare, P., Pendlbury, N., and Fraser, C.S., 2002. **'Digital orthomosaics as a source of control for geometrically correcting high resolution satellite imagery'**. Proceedings of 23rd Asian Conference on Remote Sensing, Kathmandu, Nepal.

Förstner, W. (1982) **On the Geometric Precision of Digital Correlation**. International Archives of Photogrammetry, XXIV, Part 3, 176-189.

Fraser, C.S. and Hanley, H.B., 2003. **'Bias compensation in rational functions for IKONOS satellite imagery'**. Photogramm. Engineering and Remote Sensing, 69(1): 53-57.

Grün, A.W. (1985) **Adaptive Least Squares Correlation: A Powerful Image Matching Technique**. South African Journal of Photogrammetry, Remote Sensing and Cartography, 14(3), 175-187

Grün, A.W. (1996) '**Least Squares Matching: A Fundamental Measurement Algorithm**' in Close Range Photogrammetry and Machine Vision, K. B. Atkinson (ed.) Whittles Publishing, U.K., 217-255.

Grün, A.W. & E.P. Baltsavias (1988) **Geometrically Constrained Multiphoto Matching**. Photogrammetric Engineering and Remote Sensing, 54(5), 633-641.

Heipke, C. (1992) **A Global Approach for Least Squares Image Matching and Surface Reconstruction in Object Space**. Photogrammetric Engineering and Remote Sensing, 58(3), 317-323

Mitchell, H.L. (1991) '**An Outline of Least Squares Image Matching in Digital Photogrammetry**'. First Australian Photogrammetric Conference, (University of New South Wales, Australia, 7-9 November), Paper No. 8, 10p.

Mosley, W.H., J.H. Bungey and R. Husle, 1999. '**Reinforced Concrete Design**'. 5th edition, Palgrave Houndmills, U.K.

Mustaffar, M. & Mitchell, H.L., 2001. **'Improving area-based matching by using surface gradients in the pixel co-ordinate transformation'**. ISPRS Journal of Photog. & Rem. Sensing, 56(1), pp 42-52.

Rosenholm, D. (1987a) **Multi-Point Matching Using the Least Squares Technique for Evaluation of Three-Dimensional Models**. Photogrammetric Engineering and Remote Sensing, 53(6), 621-626.

Rosenholm, D. (1987b) **Least Squares Matching Method: Some Experimental Results**. Photogrammetric Record, 12(70), 493-512.

Wolf, P.R. 1988. **'Elements of Photogrammetry'**. 2nd edition. McGraw Hill.

Wrobel, B.P. (1991) **Least-squares Methods for Surface Reconstruction From Images**. ISPRS Journal of Photogrammetry and Remote Sensing, 46, 67-84

UNIVERSITI TEKNOLOGI MALAYSIA

BORANG PENGESAHAN
LAPORAN AKHIR PENYELIDIKAN

TAJUK PROJEK : **INVESTIGATING THE FEASIBILITY OF PHOTOGRAMMETRIC AREA-BASED IMAGE MATCHING TECHNIQUE IN THE MEASUREMENT OF THREE-DIMENSIONAL DEFLECTIONS OF STRUCTURES**

Saya MUSHAIRRY MUSTAFFAR
(HURUF BESAR)

Mengaku membenarkan **Laporan Akhir Penyelidikan** ini disimpan di Perpustakaan Universiti Teknologi Malaysia dengan syarat-syarat kegunaan seperti berikut :

1. Laporan Akhir Penyelidikan ini adalah hakmilik Universiti Teknologi Malaysia.
2. Perpustakaan Universiti Teknologi Malaysia dibenarkan membuat salinan untuk tujuan rujukan sahaja.
3. Perpustakaan dibenarkan membuat penjualan salinan Laporan Akhir Penyelidikan ini bagi kategori TIDAK TERHAD.
4. * Sila tandakan (/)

☐	SULIT	(Mengandungi maklumat yang berdarjah keselamatan atau Kepentingan Malaysia seperti yang termaktub di dalam AKTA RAHSIA RASMI 1972).
☐	TERHAD	(Mengandungi maklumat TERHAD yang telah ditentukan oleh Organisasi/badan di mana penyelidikan dijalankan).
☐	TIDAK TERHAD	

TANDATANGAN KETUA PENYELIDIK

Nama & Cop Ketua Penyelidik

CATATAN : ***** *Jika Laporan Akhir Penyelidikan ini SULIT atau TERHAD, sila lampirkan surat daripada pihak berkuasa/organisasi berkenaan dengan menyatakan sekali sebab dan tempoh laporan ini perlu dikelaskan sebagai SULIT dan TERHAD.*